This file includes:

- Figures S1-S7 (incl. figure legends)

- SI References

Supplementary Figures
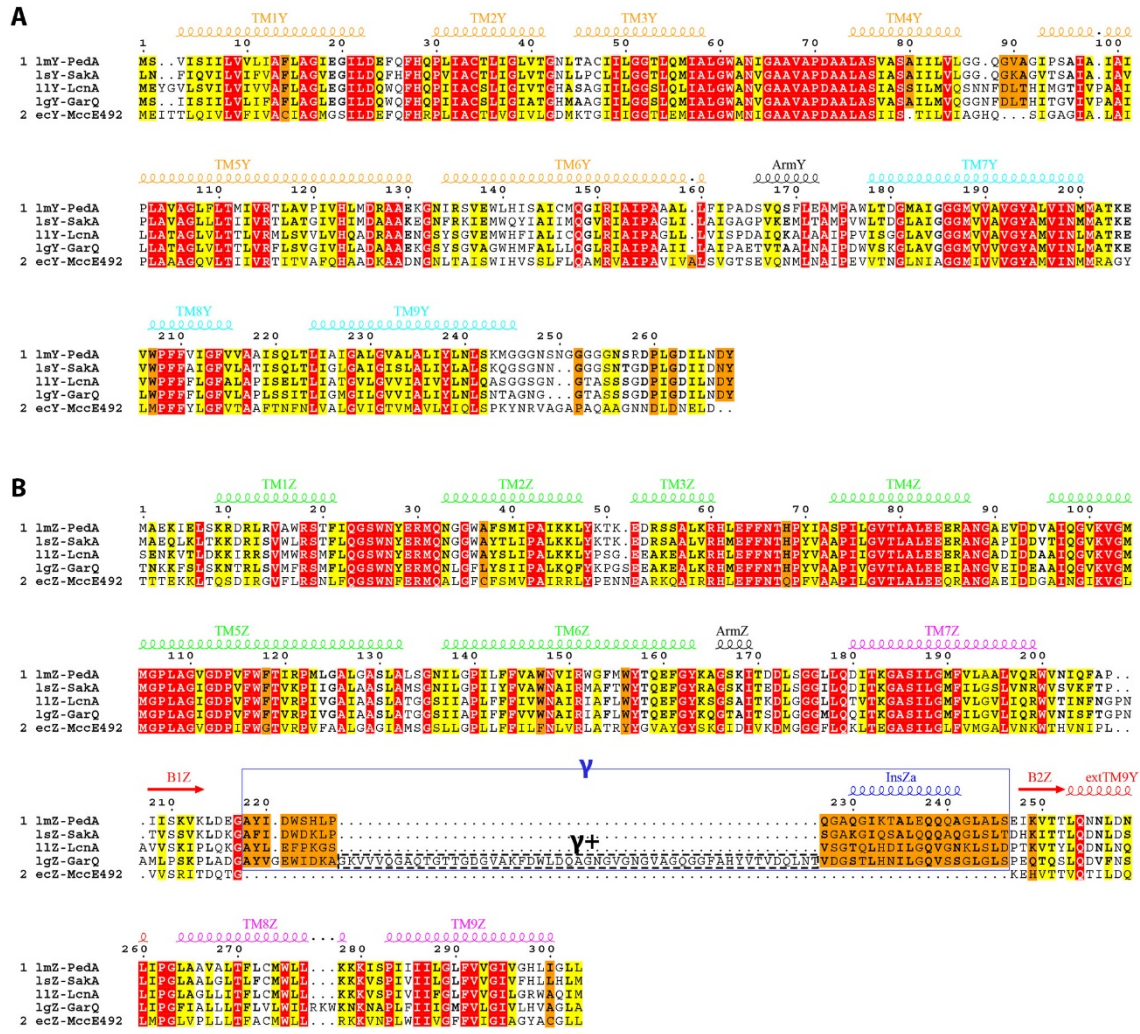

Fig. S1. **Sequence alignment of *Listeria* ManY and ManZ with homologs from other species and organisms.** The listed ManYZ homologs include that from *Listeria monocytogenes* (lm), *Latilactobacillus sakei* (ls), *Lactococcus lactis* (ll), *Lactococcus garvieae* (lg), and *E. coli* (ec). Secondary structural elements are indicated above the sequence alignment. The sequences were aligned with ClustalW (1).

(A) Sequence alignment from ManY homologs.

(B) Sequence alignment from ManZ homologs. Region γ and region γ+ specific to

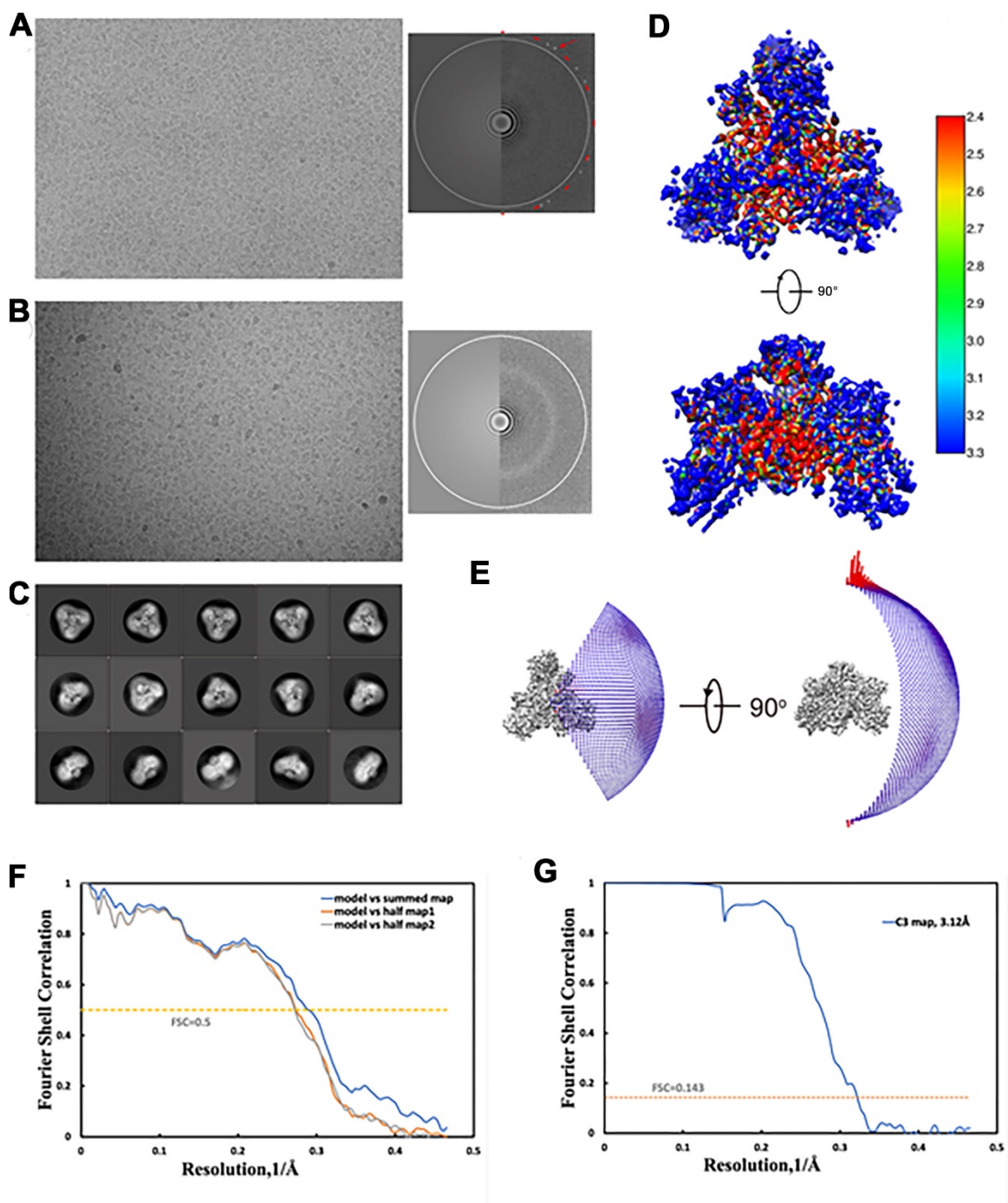*Listeria monocytogenes* and *Lactococcus garvieae* are highlighted (2, 3).

Fig. S2.   Cryo-EM analysis of bacteriocin-free man-PTS

(A) A representative cryo-EM micrograph and power spectra from the Graphene Oxide

Grid (GO), and the red arrow indicates the GO peaks.

(B) A representative cryo-EM micrograph and power spectra from the Carbon Grid. White circles indicate the estimated resolution (calculated by Gctf) of the micrographs.

(C) Representative two-dimensional class averages, with a mask diameter of 165 Å.

(D) Local-resolution maps for the 3D EM reconstruction map.

(E) Angular distribution of the particles in the final reconstruction map.

(F) Validation of the final structural model vs map.

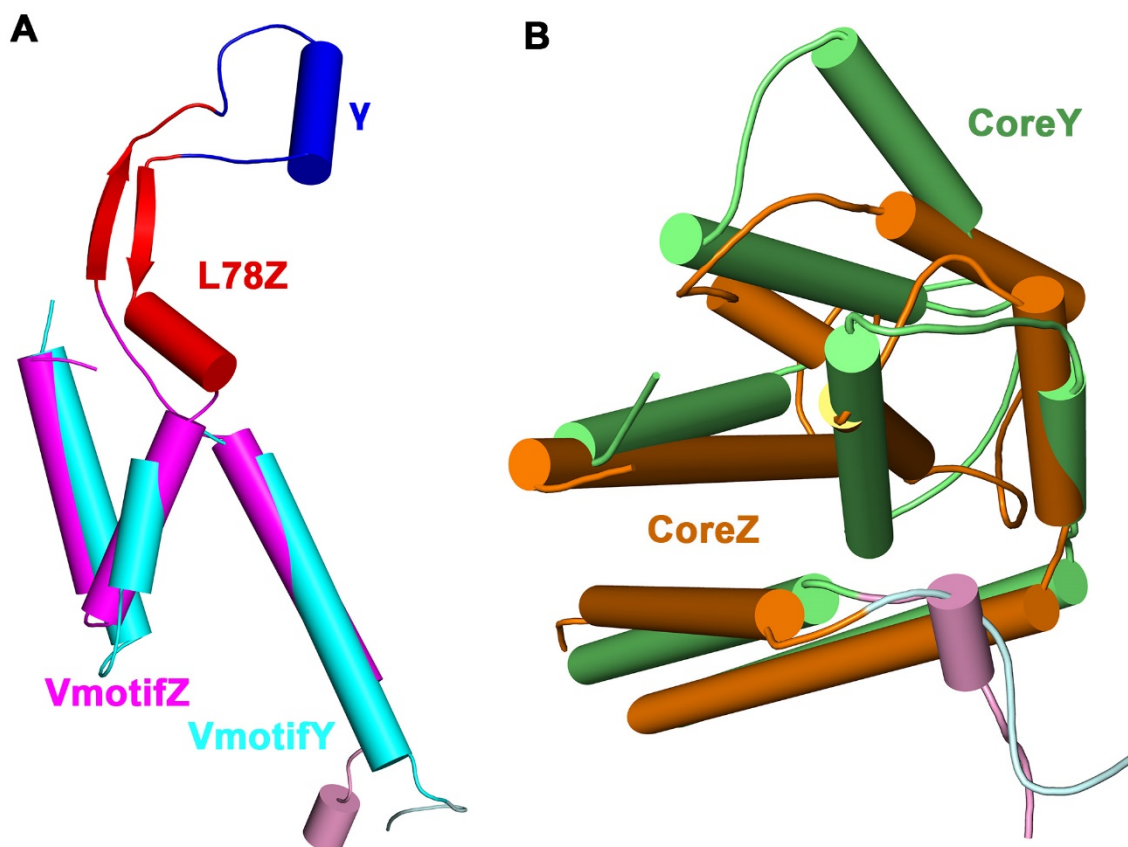(G) The gold-standard Fourier shell correlation (FSC) curve for 3D reconstruction.

Fig. S3.   **Secondary structural superposition of lmManY and lmManZ**

(A) Structural alignment of the Vmotif domain. The loop L78Z and region γ of lmManZ

   had no corresponding partners on lmManY.

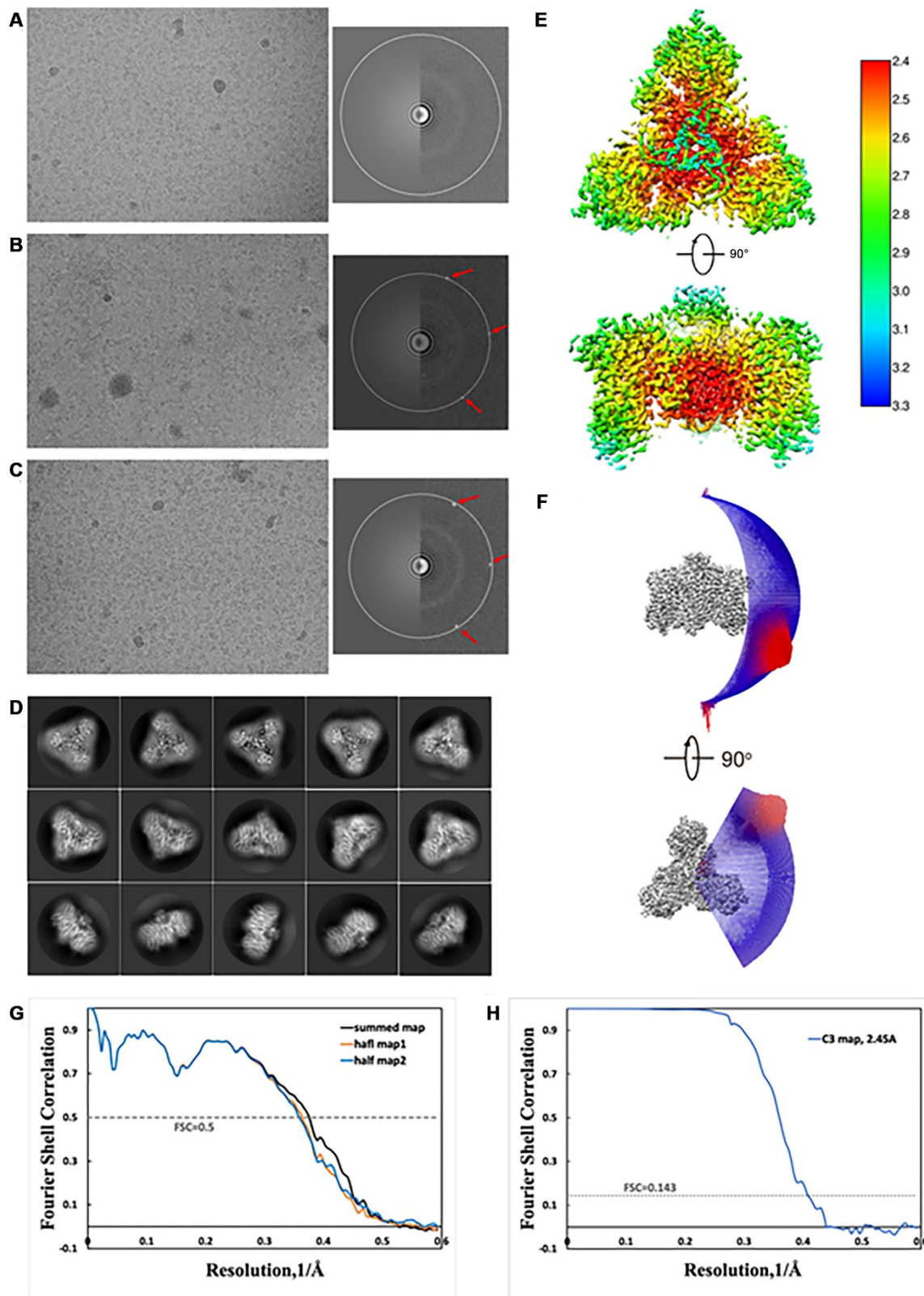(B) Structure alignment of the Core domain.

Fig. S4.   Cryo-EM analysis of the bacteriocin-bound man-PTS complex

(A) A representative cryo-EM micrograph and power spectra from a Carbon Grid.

(B) A representative cryo-EM micrograph and power spectra from the Graphene Grid, and the red arrow indicate the Graphene peaks.

(C) A representative cryo-EM micrograph and power spectra from the Graphene Oxide Grid (GO), and the red arrow indicates the GO peaks. White circles indicate the estimated resolution (calculated by Gctf) of the micrographs.

(D) Representative two-dimensional class averages, with a mask diameter of 170 Å.

(E) Local-resolution maps for the 3D EM reconstruction map.

(F) Angular distribution of the particles of the final reconstruction map.

(G) Validation of the final structure model vs map.

(H) The gold-standard Fourier shell correlation (FSC) curve for the 3D reconstruction.
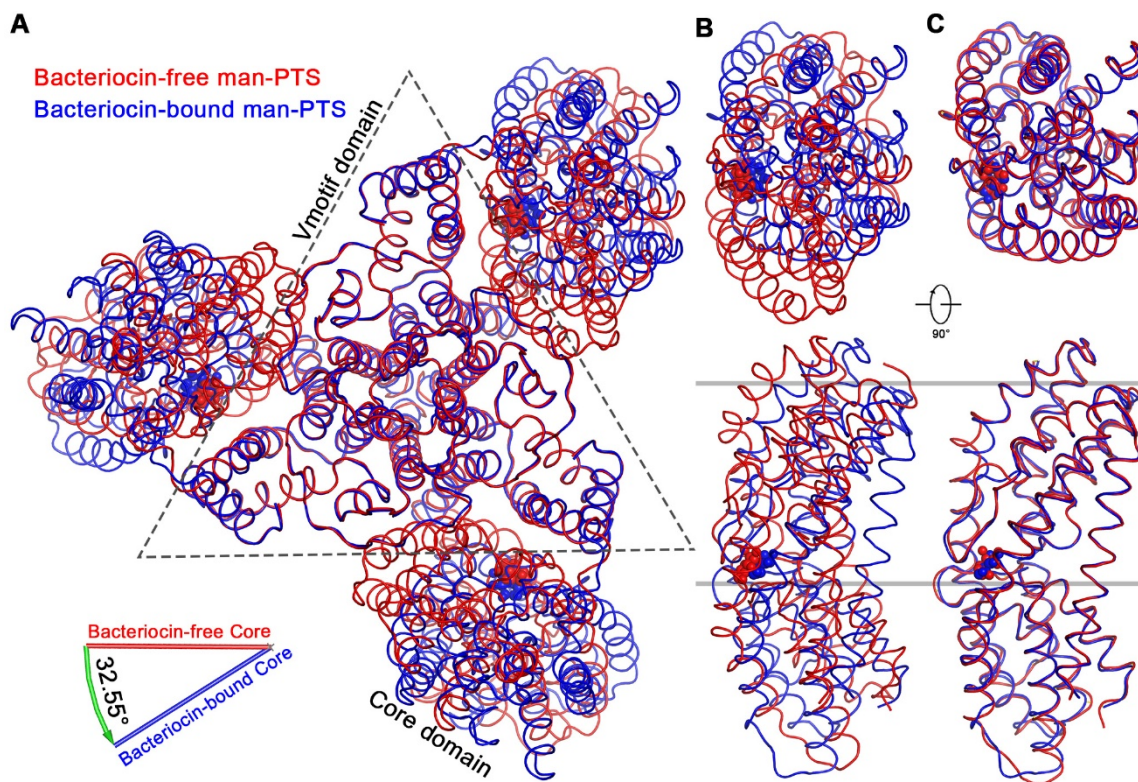
Fig. S5.   Structural comparison of the bacteriocin-free and bacteriocin-bound man-PTS

(A) Structural superposition based on the Vmotif domains. The amount and direction of rigid-body rotations between the two Core domains are indicated next to the structure.

(B) The relative orientations of the two Core domains within the membrane.

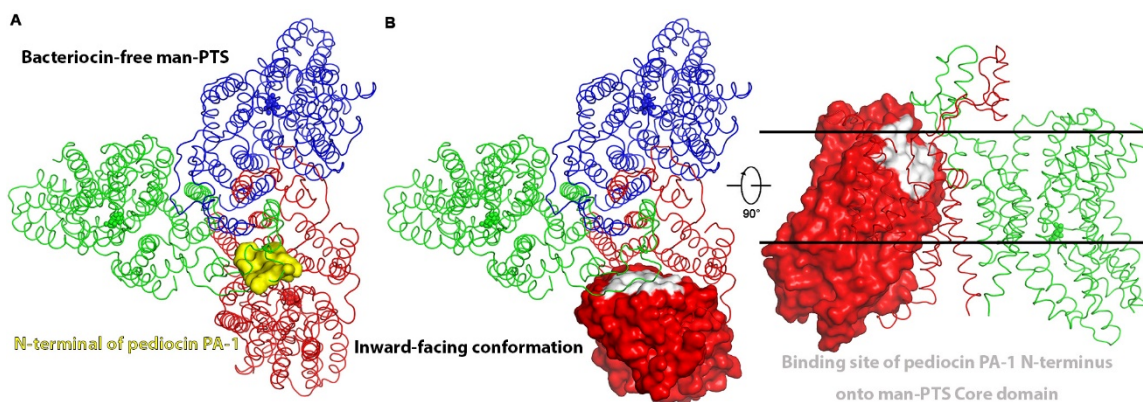(C) Alignment of Core the domains in two perpendicular views.

Fig. S6. **The possible orientation of the N-terminal region of pediocin PA-1 while binding to the bacteriocin-free man-PTS.**

(A) The bacteriocin-free man-PTS trimer is shown and colored as in Figure 1a. The N-terminal portion of pediocin PA-1 is shown in the yellow surface representation. With the current inward-facing state of bacteriocin-free man-PTS, the pediocin PA-1 N-terminal portion could not bind to the Core domain.

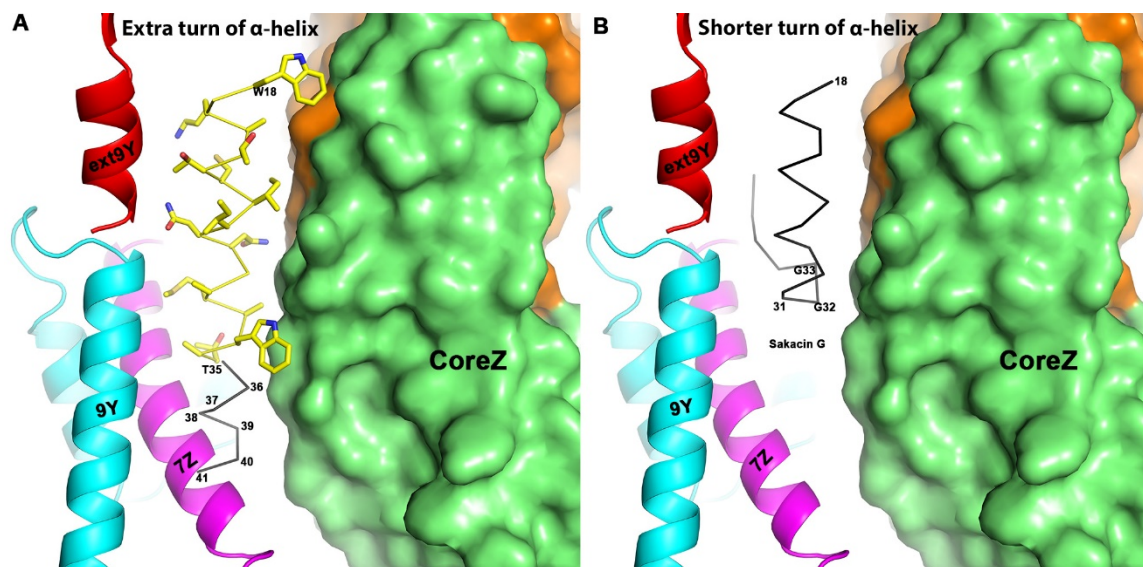(B) The binding site of the pediocin PA-1 N-terminal portion is shown as a white surface representation.

Fig. S7. **The possible configuration of the central α-helix region of PLBs with additional or fewer turns within the receptor.**

(A) One additional helical turn is modelled.

(B) Less than one turn (four residues) and the corresponding extended C-terminal tail are modelled.

References and Notes

1. Thompson JD, Gibson TJ, Higgins DG. 2002. Multiple sequence alignment using ClustalW and ClustalX. Curr Protoc Bioinformatics Chapter 2:Unit 2.3.
2. Kjos M, Nes IF, Diep DB. 2009. Class II one-peptide bacteriocins target a phylogenetically defined subgroup of mannose phosphotransferase systems on sensitive cells. Microbiology 155:2949-2961.
3. Tymoszewska A, Diep DB, Aleksandrzak-Piekarczyk T. 2018. The extracellular loop of Man-PTS subunit IID is responsible for the sensitivity of Lactococcus garvieae to garvicins A, B and C. Sci Rep 8:15790.